

Design and Screening of Ionic Liquids for C₂H₂/C₂H₄ Separation by COSMO-RS and Experiments

Xu Zhao

Key Laboratory of Biomass Chemical Engineering of Ministry of Education, Dept. of Chemical and Biological Engineering, Zhejiang University, Hangzhou 310027, China

The Institute of Seawater Desalination and Multipurpose Utilization, SOA, Tianjin 300192, China

Qiwei Yang, Dan Xu, Zongbi Bao, Yi Zhang, Baogen Su, Qilong Ren, and Huabin Xing

Key Laboratory of Biomass Chemical Engineering of Ministry of Education, Dept. of Chemical and Biological Engineering, Zhejiang University, Hangzhou 310027, China

DOI 10.1002/aic.14782

Published online March 25, 2015 in Wiley Online Library (wileyonlinelibrary.com)

Ionic liquids (ILs) have been proposed as promising solvents for separating C₂H₂ and C₂H₄, but screening an industrially attractive IL with high capacity from numerous available ILs remains challenging. In this work, a rapid screening method based on COSMO-RS was developed. We also present an efficient strategy to improve the C₂H₂ capacity in ILs together with adequate C₂H₂/C₂H₄ selectivity with the aid of COSMO-RS. The essence of this strategy is to increase molecular free volume of ILs and simultaneously enhance hydrogen-bond basicity of anions by introducing flexible and highly asymmetric structures, which is validated by a new class of tetraalkylphosphonium ILs featuring long-chain carboxylate anions. At 298.1 K and 1 bar, the solubility of C₂H₂ in ILs reaches 0.476 mol/mol IL, very high for a physical absorption, with a selectivity of up to 21.4. The separation performance of tetraalkylphosphonium ILs to the mixture of C₂H₂/C₂H₄ was also evaluated. © 2015 American Institute of Chemical Engineers AIChE J, 61: 2016–2027, 2015

Keywords: ionic liquid, acetylene, ethylene, COSMO-RS, absorption

Introduction

Acetylene/ethylene (C₂H₂/C₂H₄) separation is a very important process for the production of polymer-grade C₂H₂ or C₂H₄ in the chemical and petroleum industries.^{1–3} It is usually an energy-intensive and costly process, however, due to the similar structures and close boiling points of C₂H₂ and C₂H₄.⁴ Thus far, several methods for C₂H₄/C₂H₂ separation have been developed, such as organic solvent absorption,⁵ physical, and chemical adsorption,^{6–9} and partial hydrogenation of C₂H₂.^{10,11} Solvent absorption is one of the most popular and economical methods for C₂H₂/C₂H₄ separation in industrial applications, in which organic solvents like N, N-dimethylformamide (DMF) and N-methylpyrrolidinone (NMP) are used as absorbents to selectively capture C₂H₂.⁵ However, traditional absorption processes with organic solvents have several drawbacks, including absorbents loss, environmental pollution, and the difficulty of efficiently regenerating absorbents due to organic solvents' volatility. Therefore, there is a great need to design efficient absorbents for C₂H₂/C₂H₄ separation.

Ionic liquids (ILs) offer a new opportunity for addressing the challenge to develop novel absorbents because of their

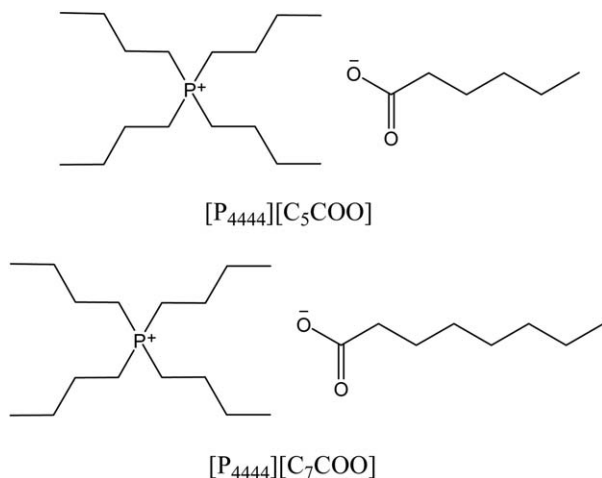
unique properties, such as negligible vapor pressures, high thermal and chemical stability, tunable structures, and properties.^{12–18} A great deal of effort has been focused on experimental and theoretical studies on the separation of C₂H₂/C₂H₄ with ILs. Different kinds of ILs, such as imidazolium-based ILs and pyrrolidinium-based ILs, have been prepared to selectively separate C₂H₂ from C₂H₄, and ILs showed superior separation selectivity over traditional organic solvents.^{19–21} The interaction mechanisms between ILs and C₂H₂ or C₂H₄ were also investigated by *ab initio* calculation and molecular dynamics simulation, and it was found that the selectivity of C₂H₂ to C₂H₄ was enhanced by increasing the hydrogen-bond basicity of ILs.^{21–23} The capacity of ILs for C₂H₂ is also a very important parameter for their industrial application, which directly relates to their economic feasibility; however, it is still a challenge task to design and screen an industrially attractive IL with high capacity and adequate selectivity from the approximately 10¹⁸ accessible ILs created from different combination of anions and cations.²⁴

The conductor-like screening model for real solvents (COSMO-RS) model developed by Klamt²⁵ is a statistical-thermodynamic model based on quantum chemistry that allows rapid *a priori* predictions of the thermodynamic properties of fluids without any experimental data. Recently, it has been used to predict the activity coefficients,^{26,27} gas solubilities,^{28–30} and separation selectivity of various gases in ILs, such as CO₂/N₂,³¹ C₂H₄/C₂H₆,³², and

Additional Supporting Information may be found in the online version of this article.

Correspondence concerning this article should be addressed to H. Xing at xinghb@zju.edu.cn.

© 2015 American Institute of Chemical Engineers



Scheme 1. The structures of quarternary phosphonium-based ILs.

$\text{H}_2\text{S}/\text{CO}_2/\text{CH}_4/\text{C}_2\text{H}_6$,³³ but there are no relevant studies on $\text{C}_2\text{H}_2/\text{C}_2\text{H}_4$ separation.

Herein, we developed an optimized COSMO-RS method to predict the Henry's law constants (K_{H}) of C_2H_4 and C_2H_2 and their separation selectivity in ILs for the first time. With the aid of COSMO-RS calculation, we designed tetraalkylphosphonium-based ILs with long-chain carboxylate anions for $\text{C}_2\text{H}_2/\text{C}_2\text{H}_4$ separation. The essence of our strategy to obtain high capacity and good selectivity of C_2H_2 in ILs is to increase the molecular free volume of ILs and enhance the hydrogen-bond (H-bond) basicity of the anion simultaneously. On the one hand, the tetraalkylphosphonium cations and long-chain carboxylate anions are both flexible and highly asymmetric, which is beneficial to the formation of cavities within ILs to accommodate more solute molecules. On the other hand, ILs with long-chain carboxylate as anions show strong H-bond basicity over common ILs, which guarantees high selectivity for C_2H_2 absorption. The solubilities of C_2H_2 , C_2H_4 , and their mixture in these tetraalkylphosphonium-based ILs (Scheme 1) at temperatures of 298.1 to 313.1 K and pressures of 20 to 160 kPa were determined in this work, and their thermodynamics and recycling performance were investigated. The IL of tetrabutylphosphonium caproate $[\text{P}_{4444}][\text{C}_5\text{COO}]$ shows excellent separation performance for C_2H_2 with a Henry's law constant K_{H} of C_2H_2 ($K_{\text{H},\text{C}_2\text{H}_2}$, the subscript denotes the name of gas) reaching 2.1 bar, which is equal to 0.476 mol C_2H_2 per mol IL at 1 bar, very high for physical absorption.

Experimental Method

Material and reagents

The 40% (wt) aqueous solution of tetrabutylphosphonium hydroxide ($[\text{P}_{4444}][\text{OH}]$) and oxazolidinone was purchased from Tokyo Chemical Industry Co. Trihexyl(tetradecyl)phosphonium bromine ($[\text{P}_{666(14)}][\text{Br}]$, $\geq 97.0\%$), acetic acid ($\geq 99.0\%$), n-hexanoic acid ($\geq 99.0\%$), n-octanoic acid ($\geq 99.0\%$), and pyrazole ($\geq 99.0\%$) were purchased from J&K scientific. 1-Butyl-3-methylimidazolium bromine was purchased from green chemistry and catalysis, LICP, CAS (China). Anion-exchange resin was obtained from Aladdin Reagent Co.(China).

Synthesis of ionic liquids

The ILs of $[\text{P}_{4444}][\text{C}_5\text{COO}]$ and tetrabutylphosphonium octoate ($[\text{P}_{4444}][\text{C}_7\text{COO}]$) were prepared as similar method reported in the literature³⁴ by neutralizing $[\text{P}_{4444}][\text{OH}]$ with equimolar n-hexanoic acid and n-octanoic acid at room temperature for 12 h. After reaction, water was distilled off at 323.1 K under reduced pressure. The IL obtained was further dried under a high vacuum at 323.1 K for at least 24 h. Other ILs with [bmim] or $[\text{P}_{666(14)}]$ (molecular structure see Table 1) as cations were prepared using the same method. The [bmim]OH, $[\text{P}_{666(14)}]\text{OH}$ solution was obtained by eluting the $[\text{P}_{666(14)}]\text{Br}$ and [bmim]Br ethanol solution through anion-exchange resin. The water contents of the ILs were determined by Karl-Fisher's titration, and the values were all below 0.3%. The structures of synthesized ILs were confirmed by NMR spectroscopy (Supporting Information).


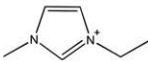
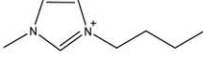
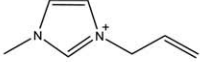
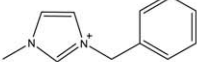
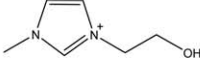
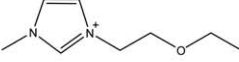
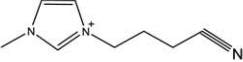
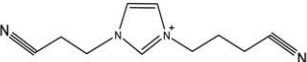
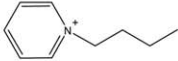
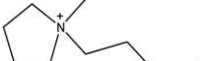
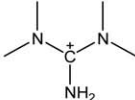
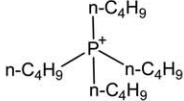
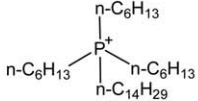
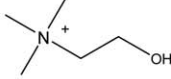
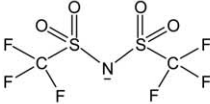
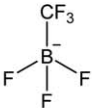
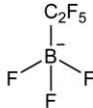
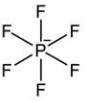
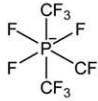
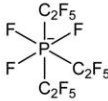
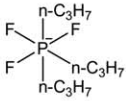
Gas solubility measurements

The solubility of C_2H_4 , C_2H_2 , and their mixture in ILs were measured by an isochoric saturation technique.^{19,21,32,35,36} The schematic diagram of the solubility measurement apparatus is shown in Figure 1, and consisted of an isothermal oven, a gas reservoir, and an equilibrium cell. The temperatures were measured with K-type thermocouples (accuracy ± 0.15 K), and pressures were determined with high precision pressure transducers (Druck RPT 350, 3.5–350 kPa, accuracy $\pm 0.01\%$ for full scale).

The experimental procedures were similar to what has been reported in the literature.^{19,21,32} A known quantity of the IL (7.0 mL) was introduced into the equilibrium cell and degassed (< 1 Pa) at 313.1 K for at least 12 h. At a specified oven temperature, the valve (V1) connecting the equilibrium cell and gas reservoir was closed to separate them. The gas was fed from the supply cylinder to the gas reservoir through V2 and V4, and then V4 was closed. The amount of the gas in the gas reservoir and line pipe at equilibrium was calculated from the pVT relation. A certain amount of target gas was brought into the equilibrium cell and mixed with the ILs by opening V1, after which V1 was closed. The IL phase was stirred vigorously with a magnetic stirrer to facilitate absorption. The equilibrium was assumed to have been reached when the pressure in the equilibration cell changed less than 1 Pa within 10 min, at which point the equilibrium pressure and temperature of the equilibrium cell and gas reservoir were recorded. For C_2H_2 – C_2H_4 binary gas mixture, the gas phase was taken out by a sealed sampler and the composition was analyzed using a SHIMADZU 2010 gas chromatograph (HP-AL/S, 50 m). After the first absorption equilibrium, valve V1 was opened again and more gas was added to the equilibration cell. Then a new equilibrium was obtained at higher pressure. By repeating these procedures, the solubility's of gases in ILs at different pressures and temperatures were measured.

The solubility of gas in the IL was calculated by subtracting the amount of gas in the pure gas phase (above the IL) at equilibrium from the total amount of gas introduced into the system. The amount of gas at a specific temperature and pressure was calculated using the gas *virial* equation of state truncated after the second term and using the second *virial* coefficients taken from the compilation by Dymond et al.³⁷ Using the solubility data, the Henry's law coefficient was obtained from the slope of a linear isotherm of fugacity vs. the mole fraction of gas in IL. The detailed calculation procedures for gas solubility were presented in Supporting Information. The reliability of this apparatus has been

Table 1. Chemical Structures of Cation and Anion Used in this Study

cation		
		
1,3-dimethylimidazolium [dmim] ⁺	1-ethyl-3-methylimidazolium [emim] ⁺	1-butyl-3-methylimidazolium [bmim] ⁺
		
1-allyl-3-methylimidazolium [amim] ⁺	1-Benzyl-3-methylimidazolium [Bnmim] ⁺	1-hydroxyethyl-3-methylimidazolium [HOemim] ⁺
		
3-(2-ethoxyethyl)-3-methylimidazolium [EtOemim] ⁺	3-(3-cyanopropyl)-3-methylimidazolium [cpmim] ⁺	1,3-di(3-cyanopropyl)imidazolium [(cp) ₂ im] ⁺
		
N-butylpyridinium [bpyr] ⁺	N-butyl-N-methylpyrrolidinium [bmpyr] ⁺	Tetramethylguanidine [tmgh] ⁺
		
Tetrabutylphosphonium [P ₄₄₄₄] ⁺	Trihexyl(tetradecyl)phosphonium [P ₆₆₆₍₁₄₎] ⁺	Choline [choline] ⁺
anion		
		
Bis(trifluoromethyl)sulfonyl [NTF ₂] ⁻	Trifluoromethyltrifluoroborate [FMB] ⁻	Pentafluoroethyltrifluoroborate [FEB] ⁻
		
Hexafluorophosphate [PF ₆] ⁻	Tris(trifluoromethyl)trifluorophosphate [FMP] ⁻	Tris(pentafluoroethyl)trifluorophosphate [FEP] ⁻
		
Tris(heptafluoropropyl)trifluorophosphate [FPrP] ⁻		

confirmed by measuring the solubility of C₂H₄ in several ILs and comparing the value with the literature results in our previous work (Supporting Information Table S1).³²

Computational Details

The molecular geometries of all compounds (cations, anions, and gaseous solutes) were optimized using TURBO-

MOLE software³⁸ at density functional theory (DFT) level, utilizing the Becke and Perdew functional^{39,40} with a triple-zeta valence polarized (TZVP)⁴¹ basis set. The COSMO files for each optimized compound were also generated by TURBOMOLE software. Then, using the COSMO file, Henry's law constants (*K_H*) of gases in ILs were calculated using the COSMOthermX program⁴² in the BP_TZVP_C30_1201 parameterization. To evaluate the reliability of DFT calculation

Table 1. Continued

Methylsulfate [MeSO ₄] ⁻	Lactate [LAc] ⁻	Imidazole [im] ⁻	Indole [ind] ⁻		
Phenolate [PhO] ⁻	Pyrazole [Pyr] ⁻	Saccharinate [SCA] ⁻	Bentrizole [Bentriz] ⁻		
Tetrazole [tetz] ⁻	Triazole [triz] ⁻	2-oxazolidinone [Oxa] ⁻	Dimethylphosphate [Me ₂ PO ₄] ⁻		
Methylphosphite [MeHPO ₃] ⁻	Ethylphosphite [EtHPO ₃] ⁻	Butylphosphite [BuHPO ₃] ⁻			
Formate [HCOO] ⁻	Acetate [OAc] ⁻	Trifluoroacetate [TFA] ⁻	Butyrate [C ₃ COO] ⁻	Caproate [C ₅ COO] ⁻	Octoate [C ₇ COO] ⁻

method, a more sophisticated *ab initio* MP2 method was also used to generate optimized geometries. In the COSMO-RS calculation, ILs are treated as an equimolar mixture of cations and anions for the sake of rapid and efficient screening. Their structures and abbreviations are listed in Table 1. The calculation theory and procedure for Henry's Law constant K_H with COSMO-RS were elaborated in Supporting Information.

The mean prediction errors (MPE) of K_H of COSMO-RS results against the experimental data^{19,20} were calculated using Eq. 1

$$\text{MPE} = \frac{1}{N} \sum_{i=1}^N \frac{|K_{H,\text{exp}} - K_{H,\text{cal}}|}{K_{H,\text{exp}}} \times 100\% \quad (1)$$

where, the $K_{H,\text{exp}}$ is the Henry's law constants (bar) of experimental data and $K_{H,\text{cal}}$ is the Henry's law constants (bar) of calculated values by COSMO-RS.

The selectivity of C_2H_2 to C_2H_4 is defined as Eq. 2

$$S_{(\text{C}_2\text{H}_2/\text{C}_2\text{H}_4)} = K_{H,\text{C}_2\text{H}_4} / K_{H,\text{C}_2\text{H}_2} \quad (2)$$

where, $K_{H,\text{C}_2\text{H}_4}$ and $K_{H,\text{C}_2\text{H}_2}$ are the Henry's law constants (bar) for C_2H_4 and C_2H_2 calculated by COSMO-RS.

Results and Discussion

Optimized COSMO-RS method

To the best of our knowledge, no COSMO-RS calculations on the solubility of C_2H_2 in ILs and the separation of C_2H_2 to C_2H_4 have been reported in the literature. Thus, the feasibility of the COSMO-RS method for screening ILs for $\text{C}_2\text{H}_2/\text{C}_2\text{H}_4$ separation was evaluated by comparing the calculated values with the experimental data. Figure 2 shows the calculated Henry's law constants of C_2H_4 and C_2H_2 in 13 kinds of ILs at 313.15 K along with their experimental data.^{19,43} It is clear that the calculated K_H values deviated significantly from the experimental values. The prediction errors is probably attributed to the diversified anion structure of investigated ILs and the weak interaction in C_2H_4 -IL systems. In this work, the experimental K_H was correlated with calculated values by linear regression (Figure 2) and the fitting results were listed in Table 2. It was found that the correlation coefficient (R^2) of $K_{H,\text{C}_2\text{H}_2}$ reached 0.94, indicating the ability of the COSMO-RS method to qualitatively predict the trend of $K_{H,\text{C}_2\text{H}_2}$ in a great variety of ILs; however, large MPE = 74.6% deriving from the overestimation of $K_{H,\text{C}_2\text{H}_2}$ were observed. COSMO-RS calculation also demonstrated

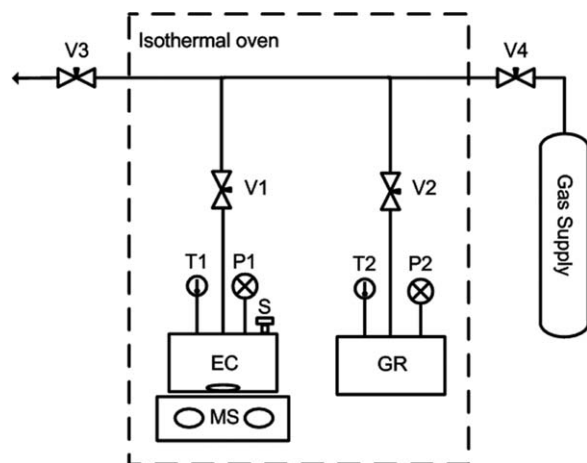


Figure 1. Schematic diagram of the solubility measurement apparatus: (EC) equilibrium cell, (GR) gas reservoir, (V1–4) valves, (T1–2) K-type thermocouples, (P1–2) pressure transducer, (S) sampling valve, and (MS) magnetic stirrer.

obvious deviations in the prediction of K_{H,C_2H_4} ($R^2 = 0.36$, MPE = 33.2%). The predicted selectivity of C_2H_2 to C_2H_4 calculated by the ratio of K_{H,C_2H_2} to K_{H,C_2H_4} produced a larger deviation ($R^2 = 0.36$, MPE = 211%) due to the accumulation of error. Therefore, to providing a reliable methodology for screening ILs for C_2H_2/C_2H_4 separation, it is necessary to correct and optimize the COSMO-RS method.

As shown by the data in Figure 2, one of the main predictive errors stemmed from the overestimation of the value of K_H . Thus, the equations obtained from linear regression (Table 2) were adopted to correct the COSMO-RS calculation. The equations for correction were shown as Eqs. 3 and 4. Ortiz and coworkers also used a similar method to improve the prediction performance of COSMO-RS for propane/propylene in ILs.⁴⁴

$$K_{H,C_2H_4,opt-cal} = 1.46 \times K_{H,C_2H_4,cal} + 11.7 \quad (3)$$

$$K_{H,C_2H_2,opt-cal} = 1.76 \times K_{H,C_2H_2,cal} + 4.56 \quad (4)$$

The prediction results with the optimized COSMO-RS method are shown in Figure 3 and Table 2. It is clear that the calculated K_H of C_2H_4 and C_2H_2 both agree with the experimental results. Although the correlation coefficients are kept constant with this optimized method, the MPE for C_2H_4 decreased from 33.2 to 23.1% and that for C_2H_2 decreased from 74.6 to 12.7%. Accordingly, the calculated selectivity of C_2H_2 to C_2H_4 with the optimized method was also greatly improved. The R^2 of selectivity increased from 0.36 to 0.78, and the MPE of selectivity decreased from 211 to 26.1%. The improvement in predicting selectivity is represented more visually in Figure 4. The systemic error of COSMO-RS prediction for K_H and selectivity was corrected by this optimized method. Thus, it is feasible that the optimized COSMO-RS calculation can predict the K_H and selectivity of C_2H_2 in various ILs.

In this work, MP2 method was also used for calculation and the results were presented in Supporting Information Figures S1 and S2. As shown in Supporting Information Figures S1, S2 and Figure 2, 3, there was no obvious difference on the value of calculated K_{H,C_2H_4} , K_{H,C_2H_2} , and optimized selectivity of C_2H_2 to C_2H_4 between MP2 and DFT method. The MPE of calculated K_{H,C_2H_4} and K_{H,C_2H_2} by MP2 and DFT

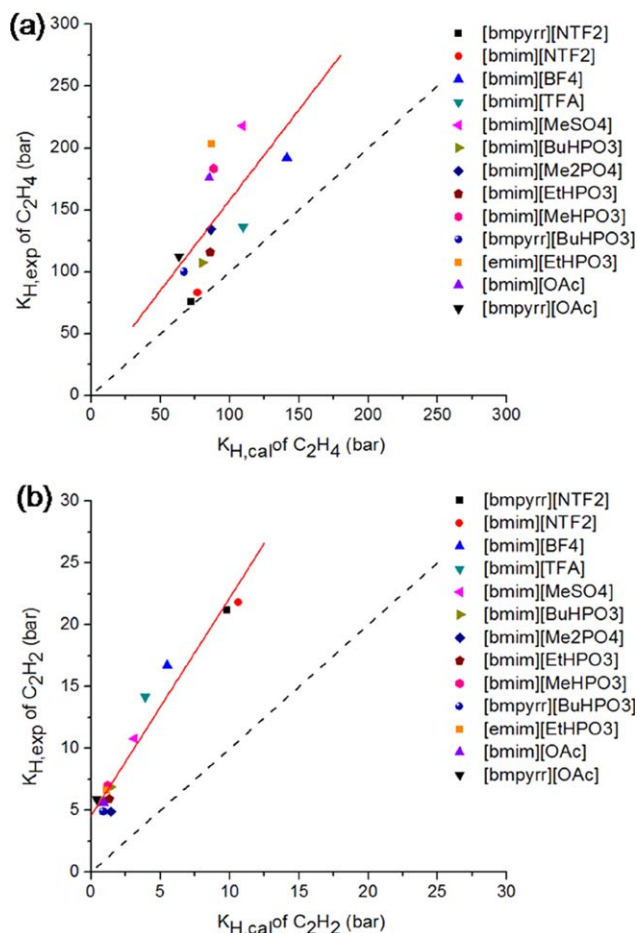


Figure 2. Comparison between the experimental and COSMO-RS calculated Henry's law constants of C_2H_4 (a) and C_2H_2 (b) at 313.15 K.

[Color figure can be viewed in the online issue, which is available at [wileyonlinelibrary.com](http://www.interscience.wiley.com).]

method was 34.8, 67.1 33.2, and 74.6%, respectively. (Supporting Information Figures S1, S2). Considering both computation accuracy and computation time, DFT method was adopted in this work.

Screening the ILs to separate C_2H_2 from C_2H_4

In this work, various classic cations, including 1-alkyl-3-alkylimidazolium with different lengths of alkyl chains and functional groups, 1-butyl-1-methylpyrrolidinium ([bmpyrr]⁺), and N-butylpyridinium ([bpyr]⁺), and classic anions, including bis(trifluoromethylsulfonyl)imide anion ([NTF2][−]), fluorinated

Table 2. Statistical Results Obtained from the Comparison of Experimental and Predicted Henry's Law Constants (K_H /bar of C_2H_4 , C_2H_2 , and Their Selectivities ($S_{(C_2H_2/C_2H_4)}$) in ILs

Model		Slope	y-intercept	R^2	MPE (%)
COSMO-RS	K_{H,C_2H_4}	1.46	11.7	0.36	33.2
	K_{H,C_2H_2}	1.76	4.56	0.94	74.6
	$S_{(C_2H_2/C_2H_4)}$	0.15	9.74	0.36	211
Optimized COSMO-RS	K_{H,C_2H_4}	1.00	0.03	0.36	23.1
	K_{H,C_2H_2}	1.00	−0.06	0.94	12.7
	$S_{(C_2H_2/C_2H_4)}$	1.52	−6.95	0.78	26.1

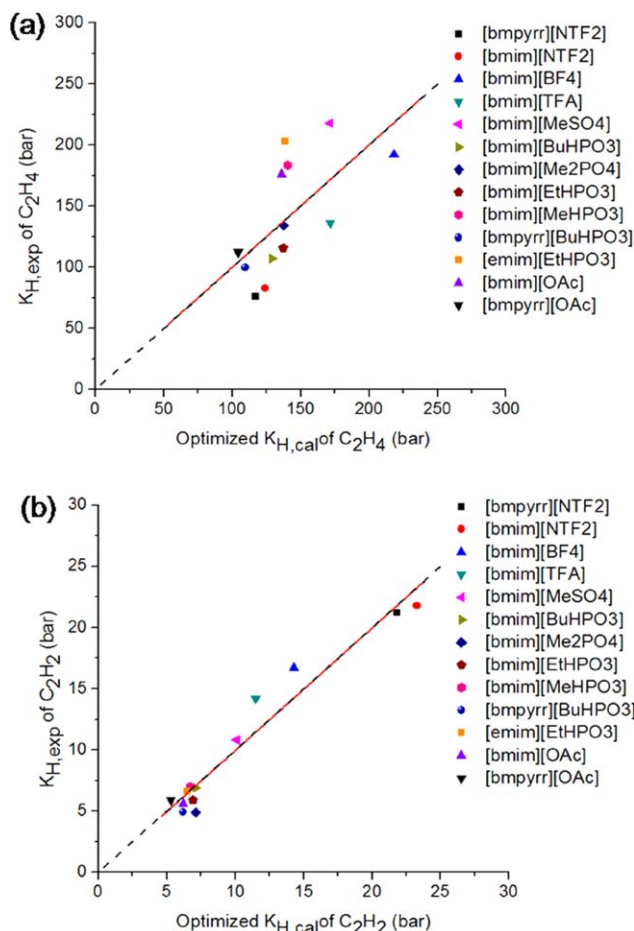


Figure 3. Comparison between the experimental and optimized COSMO-RS calculated Henry's law constants of C_2H_4 (a) and C_2H_2 (b) at 313.15 K.

[Color figure can be viewed in the online issue, which is available at wileyonlinelibrary.com.]

tetrafluoroborate derivatives (FMB^- , FEB^-), hexafluorophosphate anion ($[PF_6]^-$) and its fluorinated derivatives (FMP^- , FEP^- , $FPrP^-$), were selected to constitute ILs for evaluation. In particular, with the aim of designing a suitable IL with high capacity and satisfactory separation selectivity, phosphonium cations ($[P_{4444}]^+$, $[P_{666(14)}]^+$) with a large molecular free volume, functionalized guanidinium cations with basic sites ($[tmgh]^+$), and carboxylate and phosphate anions with different alkyl chain lengths, and heterocycle anions with strong basic sites, were considered in the screening calculation. Combining the aforementioned 15 cations and 28 anions (their structures are shown in Table 1), 420 ILs were constituted and evaluated using the optimized COSMO-RS approach. The calculated K_H of C_2H_4 and C_2H_2 in 420 ILs at 313.15 K are listed in Supporting Information Tables S2 and S3.

As shown in Figure 5, the $S_{(C_2H_2/C_2H_4)}$ depended mainly on the type of anion. Overall, the ILs with anions showing strong H-bond basicity (H-bond acceptor ability) all perform satisfactory selectivity, such as carboxylate, phosphate, oxazolidinone, triazole, tetrazole, and so forth. Among these anions, the carboxylate anions ($[C_7COO]^- \sim [OAc]^-$) on the left side of Figure 4 show satisfactory selectivity ($S_{(C_2H_2/C_2H_4)}$ are above 24), which are obviously superior to

the common anions, such as $[NTF_2]^-$, $[PF_6]^-$, $[FMB]^-$, $[FEB]^-$, and $[FPrP]^-$.

Besides selectivity, the absorption capacity of the solute in an absorbent is also a very important parameter for industrial applications. Therefore, the mole fraction of C_2H_2 in ILs was treated as another screening index. As shown in Figure 6, the type of anion still has a significant effect on the capacity of C_2H_2 in ILs. For example, the calculated capacity of ILs with $[bmim]^+$ as cations have following order: carboxylate > phosphate > [Oxa] > [triz] >> [im] > [ind] >> $[FEB]^- > [PF_6]^- > [FEP]^-$. ILs with anions having strong H-bond basicity and a bulky and flexible structure, such as long-chain carboxylate anions, show a relatively high capacity for C_2H_2 . However, the anions of [triz], [ind], and [im], which have a strong H-bond basicity but a rigid structure, demonstrate moderate absorption capacity. Nor is it surprising that the calculated capacity of ILs with weak H-bond basicity is low. It is very interesting that we found the structures of cations also play an important role in determining the C_2H_2 capacity of ILs. The calculated molar capacities of ILs with tetraalkylphosphonium, $[P_{4444}]^+$, $[P_{666(14)}]^+$, 1-butyl-1-methylpyrrolidinium ($[bmpyr]^+$), and tetramethylguanidine ($[tmgh]^+$) as cations are significantly larger than

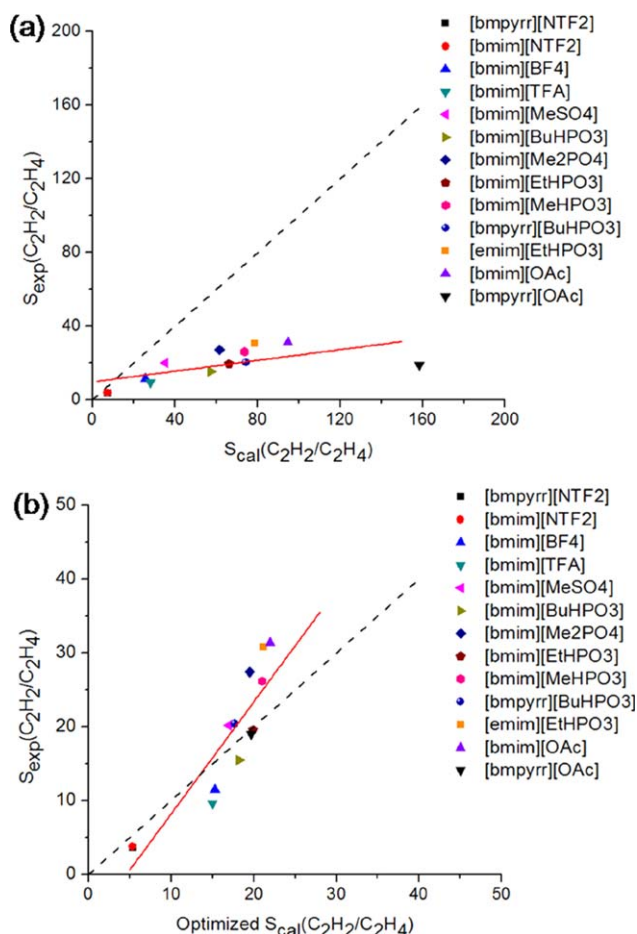


Figure 4. Comparison between the experimental and predicted C_2H_2/C_2H_4 selectivities at 313.15 K, using Henry's law constants predicted by (a) standard COSMO-RS and (b) optimized COSMO-RS.

[Color figure can be viewed in the online issue, which is available at wileyonlinelibrary.com.]

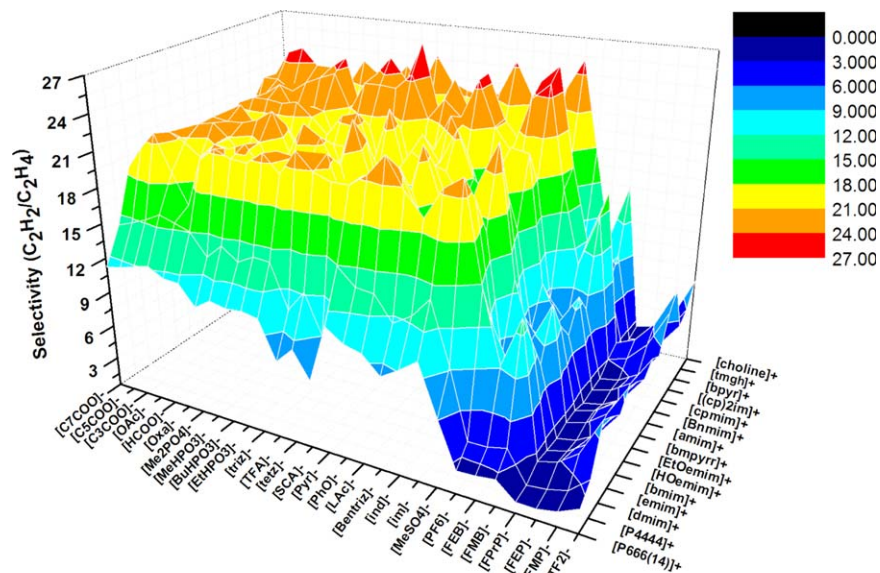


Figure 5. Prediction of C_2H_2/C_2H_4 selectivity in 420 ILs at $T = 313.15$ K calculated by optimized COSMO-RS approach.

[Color figure can be viewed in the online issue, which is available at wileyonlinelibrary.com.]

that of imidazolium-based ILs (Figure 6). The high calculated capacities of ILs with bulky cations, such as $[P_{4444}]^+$, $[P_{666(14)}]^+$, and $[bmpyrr]^+$, were probably due to their relatively large molecular free volume. Additionally, the larger capacity of $[tmgh]^+$ -based ILs may be owing to the strong polarity of the guanidinium cation. In particular, the combination of phosphonium cations ($[P_{4444}]^+$, $[P_{666(14)}]^+$) with carboxylate anions have the greatest molar capacity of C_2H_2 , which is more than 0.185 at 1 bar and 313.15 K.

Evaluation on ILs

According to the results of COSMO-RS calculation, four cations, including $[P_{4444}]^+$, $[P_{666(14)}]^+$, $[bmpyrr]^+$ and $[tmgh]^+$, and five anions with strong H-bond basicity ($[OAc]^-$,

$[C_3COO]^-$, $[C_5COO]^-$, $[C_7COO]^-$, $[Oxa]^-$, and $[Pyr]^-$) that have good calculated selectivity and capacity, were selected as ions to constitute possible available ILs for experimental evaluation. However, $[P_{4444}]$ -based ILs with short-chain carboxylate anions ($[OAc]^-$ and $[C_3COO]^-$) are solid at room temperature, and ILs with $[tmgh]^+$ as cation are very viscous liquids or even solids at room temperature. Therefore, those ILs are not suitable for gas separation. Thus, five phosphonium-based ILs, including $[P_{4444}][C_5COO]$, $[P_{4444}][C_7COO]$, $[P_{666(14)}][OAc]$, $[P_{666(14)}][Pyr]$, and $[P_{666(14)}][Oxa]$, were prepared and their separation performances were evaluated by experimental measurements of K_{H,C_2H_2} and K_{H,C_2H_4} . The K_{H,C_2H_2} and K_{H,C_2H_4} in $[bmim][C_5COO]$ and $[bmim][C_7COO]$ were also measured in this work for comparison. In

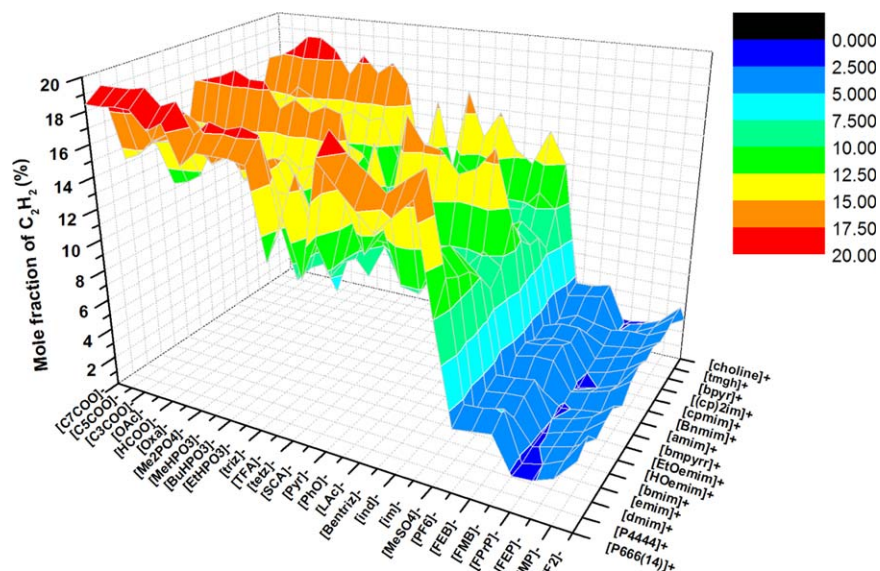


Figure 6. Prediction of C_2H_2 capacity in 420 ILs at $T = 313.15$ K, $P = 1$ bar calculated by optimized COSMO-RS approach.

[Color figure can be viewed in the online issue, which is available at wileyonlinelibrary.com.]

Table 3. Henry's Law Constants (K_H) of C_2H_4 , C_2H_2 and Their Ideal Selectivity (S) in ILs

ILs	β	T/K	K_H/bar^a C_2H_4	K_H/bar^a C_2H_2	S^b C_2H_2/C_2H_4
[P ₄₄₄₄][C ₅ COO]	1.486	298.1	44.9 (± 0.1)	2.1 (± 0.1)	21.4
		303.1	48.8 (± 0.1)	2.4 (± 0.1)	20.3
		308.1	51.4 (± 0.2)	2.9 (± 0.1)	17.7
		313.1	53.6 (± 0.1)	3.3 (± 0.1)	16.2
[P ₄₄₄₄][C ₇ COO]	1.548	298.1	40.3 (± 0.2)	2.3 (± 0.1)	17.5
		303.1	44.8 (± 0.1)	2.6 (± 0.1)	17.2
		308.1	47.1 (± 0.2)	3.0 (± 0.1)	15.7
		313.1	48.5 (± 0.1)	3.5 (± 0.1)	13.9
[bmim][C ₅ COO]	1.267	298.1	89.6 (± 1.1)	4.2 (± 0.1)	21.3
		303.1	96.8 (± 0.4)	4.8 (± 0.1)	20.2
		308.1	100.4 (± 0.3)	5.6 (± 0.1)	17.9
		313.1	104.9 (± 0.7)	6.3 (± 0.1)	16.7
[bmim][C ₇ COO]	1.379	298.1	71.6 (± 0.4)	4.3 (± 0.1)	16.7
		303.1	77.3 (± 0.3)	5.0 (± 0.1)	15.5
		308.1	80.4 (± 0.2)	5.8 (± 0.1)	13.9
		313.1	85.7 (± 0.2)	6.7 (± 0.1)	12.8
[P ₆₆₆₍₁₄₎][OAc]		298.1	29.0 (± 0.1)	3.1 (± 0.1)	9.4
		303.1	32.1 (± 0.1)	3.5 (± 0.1)	9.2
		308.1	33.9 (± 0.1)	3.9 (± 0.1)	8.7
		313.1	34.2 (± 0.1)	4.6 (± 0.1)	7.4
[P ₆₆₆₍₁₄₎][Pyr]		313.1		8.9 (± 0.1)	
[P ₆₆₆₍₁₄₎][Oxa]		313.1		6.4 (± 0.1)	
[bmim][BF ₄] ^c	0.376	313.1	192.2 (± 3.4)	17.5 (± 0.1)	11.0
[bmim][OAc] ^c	1.090	313.1	175.9 (± 1.6)	6.4 (± 0.1)	27.5
[bmpyrr][OAc] ^c		313.1	112.3 (± 2.3)	5.9 (± 0.2)	19.0
[bmim][MeHPO ₃] ^c		313.1	183.4 (± 1.3)	7.1 (± 0.1)	25.8

^aValues in bracket are the slope errors of the linear isotherms.

^b $K_{H,C_2H_4}/K_{H,C_2H_2}$

^cData is from reference 19.

the process of naphtha and natural gas cracking, although the total pressure of the cracking gas reaches 0.8 MPa, the partial pressure of C_2H_2 or C_2H_4 is below 0.1 MPa. Thus, in this work, the solubility of C_2H_2 and C_2H_4 in ILs was determined at pressures from approximately 20 to 160 kPa and at temperatures of 298.1, 303.1, 308.1 and 313.1 K. The solubility data are presented in Supporting Information Table S4. The K_{H,C_2H_2} and K_{H,C_2H_4} representing the gas solubility in ILs were obtained from the slope of the linear isotherm of fugacity vs. molar fraction; the results are listed in Table 3. The molar solubility of gas has a reciprocal relationship with the value of K_H . The low value of K_H means greater solubility.

As shown in Table 3, high C_2H_2 capacity and satisfactory selectivity were both achieved with [P₄₄₄₄][C₅COO] and [P₄₄₄₄][C₇COO] as absorbents. The K_{H,C_2H_2} of [P₄₄₄₄][C₅COO] and [P₄₄₄₄][C₇COO] reached 3.3 and 3.5 bar at 313.1 K, respectively. It is significantly lower than that in previously reported ILs ([bmim][BF₄]: 17.5, [bmim][MeHPO₃]: 7.1, [bmim][OAc]: 6.4, and [bmpyrr][OAc]: 5.9) at the same temperature,¹⁹ indicating improved capacities of ILs for C_2H_2 absorption. When the temperature decreased to 298.1 K, the K_{H,C_2H_2} of [P₄₄₄₄][C₅COO] and [P₄₄₄₄][C₇COO]

further dropped to 2.1 and 2.3 bar, respectively. It means that near 2-mol ILs could capture 1-mol C_2H_2 at 1 bar. The high capacities of [P₄₄₄₄][C₅COO] and [P₄₄₄₄][C₇COO] were partially attributed to the characteristics of long-chain carboxylate anions. The [C₅COO][−] anion has a very high H-bond basicity (β) compared with other anions and the value of β of [P₄₄₄₄][C₅COO] is up to 1.486. As we know, [OAc][−] is regarded as a strong basic anion; however, the β value of [bmim][OAc] is only 1.090. Besides the influence of anions, the [P₄₄₄₄]⁺ cation also made a great contribution to the large C_2H_2 capacity, which can be observed from the comparison between [P₄₄₄₄]-based ILs and [bmim]-based ILs with the same anion (Table 3). The K_{H,C_2H_2} was 2.1 bar with [P₄₄₄₄][C₅COO] at 298.1 K; however, the value increased to 4.2 bar in [bmim][C₅COO] at the same temperature. This means that the molar solubility of C_2H_2 in ILs with [C₅COO] as the same anion could be doubled when the cation was changed from [bmim] to [P₄₄₄₄]. The reasons can be attributed to the two major effects. First, the molecules of [P₄₄₄₄]⁺ are much larger in size than [bmim]⁺, which not only strengthens the van der Waals interaction between IL and organic C_2H_2 molecule but also benefits the formation of cavities within ILs to accommodate more solute

Table 4. Coefficients of Eq. 5(5) and the Percent Average Absolute Deviation (AAD) of the Fit

ILs	C_2H_4				C_2H_2			
	B_0	B_1	B_2	AAD	B_0	B_1	B_2	AAD
[P ₄₄₄₄][C ₅ COO]	−27.8	2.05×10^4	$−3.29 \times 10^6$	0.14	16.9	$−6.84 \times 10^3$	6.041×10^5	0.02
[P ₄₄₄₄][C ₇ COO]	−60.6	4.05×10^4	$−6.35 \times 10^6$	0.10	47.7	$−2.59 \times 10^4$	3.556×10^6	0.01
[bmim][C ₅ COO]	−20.9	1.65×10^4	$−2.66 \times 10^6$	0.02	4.22	9.85×10^2	$−5.412 \times 10^5$	0.01
[bmim][C ₇ COO]	−1.04	4.38×10^3	$−8.34 \times 10^5$	0.01	13.6	$−4.55 \times 10^3$	2.725×10^5	0.05
[P ₆₆₆₍₁₄₎][OAc]	−76.4	4.98×10^4	$−7.77 \times 10^6$	0.14	57.3	$−3.18 \times 10^4$	4.485×10^6	0.02

Table 5. Gibbs Free Energy, Enthalpy, and Entropy of Solvation for C₂H₄ and C₂H₂ in ILs at Different Temperatures ($p^0 = 1$ bar)

T/K	$\Delta_{\text{solv}}G$ (kJ·mol ⁻¹)	$\Delta_{\text{solv}}H$ (kJ·mol ⁻¹)	$\Delta_{\text{solv}}S$ (J·mol ⁻¹ ·K ⁻¹)	$\Delta_{\text{solv}}G$ (kJ·mol ⁻¹)	$\Delta_{\text{solv}}H$ (kJ·mol ⁻¹)	$\Delta_{\text{solv}}S$ (J·mol ⁻¹ ·K ⁻¹)
[P ₄₄₄₄][C ₅ COO]–C ₂ H ₄				[P ₄₄₄₄][C ₅ COO]–C ₂ H ₂		
298.1	9.4	–13.5	–76.8	1.8	–23.2	–83.9
303.1	9.8	–10.4	–66.7	2.2	–23.7	–85.6
308.1	10.1	–7.5	–57.1	2.7	–24.3	–87.6
313.1	10.4	–4.7	–48.0	3.1	–24.8	–89.1
[P ₄₄₄₄][C ₇ COO]–C ₂ H ₄				[P ₄₄₄₄][C ₇ COO]–C ₂ H ₂		
298.1	9.2	–17.9	–90.8	2.1	–17.0	–64.0
303.1	9.6	–12.1	–71.4	2.4	–20.3	–74.9
308.1	9.9	–6.4	–52.8	2.8	–23.4	–85.2
313.1	10.1	–0.9	–35.2	3.3	–26.5	–95.1
[bmim][C ₅ COO]–C ₂ H ₄				[bmim][C ₅ COO]–C ₂ H ₂		
298.1	11.1	–11.5	–75.9	3.6	–22.0	–85.7
303.1	11.5	–9.0	–67.8	4.0	–21.5	–84.0
308.1	11.8	–6.7	–59.9	4.4	–21.0	–82.5
313.1	12.1	–4.4	–52.6	4.8	–20.6	–80.9
[bmim][C ₇ COO]–C ₂ H ₄				[bmim][C ₇ COO]–C ₂ H ₂		
298.1	10.6	–10.1	–69.4	3.6	–22.6	–87.9
303.1	11.0	–9.3	–66.9	4.1	–22.8	–88.7
308.1	11.2	–8.6	–64.3	4.5	–23.1	–89.5
313.1	11.6	–7.9	–62.1	5.0	–23.3	–90.3
[P ₆₆₆₍₁₄₎][OAc]–C ₂ H ₄				[P ₆₆₆₍₁₄₎][OAc]–C ₂ H ₂		
298.1	8.3	–18.9	–91.5	2.8	–14.1	–56.5
303.1	8.7	–11.8	–67.7	3.2	–18.2	–70.4
308.1	9.0	–4.9	–45.0	3.5	–22.2	–83.3
313.1	9.2	1.8	–23.5	4.0	–26.0	–95.8

molecules. Secondly, it was found that the basicity of ILs with the same anion could be enhanced when the cation–anion interaction was weakened and the value of β increased by 29% when the cation changed from [bmim] to [P₄₄₄₄].⁴⁵ Consequently, the affinity of the anion in [P₄₄₄₄]-based ILs toward C₂H₂ is believed to be strengthened compared with that in [bmim]-based ILs.

The [P₄₄₄₄][C₅COO] and [P₄₄₄₄][C₇COO] also displayed good selectivity to C₂H₂. The value of $S_{(\text{C}_2\text{H}_2/\text{C}_2\text{H}_4)}$ was up to 16.2 and 21.4 in [P₄₄₄₄][C₅COO] at 313.1 and 298.1 K, respectively, which was clearly greater than [bmim][BF₄] (11.0, 313.1K) but lower than [bmppyr][OAc] (19.0, 313.1K), [bmim][MeHPO₃] (25.8, 313.1K) and [bmim][OAc] (27.5, 313.1 K). The $S_{(\text{C}_2\text{H}_2/\text{C}_2\text{H}_4)}$ of [P₄₄₄₄][C₅COO] was satisfactory for industrial applications because the required number of theoretical plates was about 15 at 298.1 K for a complete separation of C₂H₂ and C₂H₄ based on the classic absorption theory. In addition, the experimental results are in agreement with the prediction results, such that $K_{\text{H,C}_2\text{H}_2}$ is [P₄₄₄₄][C₅COO] \approx [P₄₄₄₄][C₇COO] < [P₆₆₆₍₁₄₎][OAc] < [bmim][C₅COO] \approx [bmim][C₇COO], and $K_{\text{H,C}_2\text{H}_4}$ is [P₆₆₆₍₁₄₎][OAc] < [P₄₄₄₄][C₅COO] \approx [P₄₄₄₄][C₇COO] < [bmim][C₅COO] \approx [bmim][C₇COO], indicating the COSMO-RS screening method proposed in this work is reliable.

Several anions with strong H-bond basicity, such as [OAc][–], [C₃COO][–], [Pyr][–], and [Oxa][–], were also investigated in this work. However, the combination of [P₄₄₄₄]⁺ and the aforementioned anions are solid at room temperature due to their rigid and symmetric molecular structure. To prepare room temperature ILs, [P₆₆₆₍₁₄₎]⁺, which has a more flexible and asymmetric structure compared with [P₄₄₄₄]⁺, was selected as the cation; however, as shown in Table 3, the selectivity of C₂H₂ to C₂H₄ in [P₆₆₆₍₁₄₎][OAc] is less than 10 at 298.1 K. This may be attributed to the excessive molecular size of the [P₆₆₆₍₁₄₎]⁺ cation.

Another advantage of [P₄₄₄₄][C₅COO] is its relatively low viscosity. The viscosity of [P₄₄₄₄][C₅COO] at 338.15 K is

43.6 mPa s, only slightly higher than [bmim][OAc] (34.7 mPa s) but significantly lower than other strong basic ILs, such as [P₄₄₄₄][Pyr] and [P₄₄₄₄][Oxa].⁴⁶ Therefore, [P₄₄₄₄][C₅COO] demonstrates a fast absorption rate (Supporting Information Figure S3). At present, organic solvents DMF and NMP are the most popular absorbents for the separation of C₂H₂ in industrial processes.⁵ Compared with DMF and NMP, [P₄₄₄₄][C₅COO] not only clearly enhances C₂H₂ selectivity, achieving 21.4 at 298.1K, but also exhibits greatly increased molar and mass solubilities.⁴⁷ The solubility of C₂H₂ in [P₄₄₄₄][C₅COO] is 0.476 bar^{–1} in mole fraction and 2.425 mol kg^{–1} bar^{–1} for mass capacity, respectively, which is four times larger than the molar solubilities of DMF and NMP (0.099 and 0.104 bar^{–1}, respectively),⁴⁷ and near double the mass capacity of DMF and NMP (1.501 and 1.319 mol kg^{–1} bar^{–1}, respectively).⁴⁷ It is worth mentioning that the molar solubility of C₂H₂ in [P₄₄₄₄][C₅COO] is very high and the value reaches 0.476 mol C₂H₂ per mol ILs at 1 bar, which is unusually high for common physical absorption processes. This can probably be attributed to the relatively high free volume of ILs and their very strong H-bond basicity. Thus, considering its excellent capacity and selectivity, [P₄₄₄₄][C₅COO] shows great potential in separating C₂H₂ from C₂H₄.

Temperature dependent gas solubility

Generally, Henry's law constants of gas solutes in ILs can be correlated by an empirical formula of the type^{48–53}

$$\ln(K_{\text{H}}) = \sum_{i=0}^n B_i T^{-i} \quad (5)$$

where, K_{H} is the Henry's law constants (bar) at a certain temperature (K) and B_i ($i = 0-2$) is the fitting coefficients. The value of B_i as well as the average absolute deviation of the fit are listed in Table 4.

Table 6. Real Henry's Law Constants (K_H) and Real Selectivity of C_2H_2 – C_2H_4 Mixtures in $[P_{4444}][C_5COO]$

Solute	T/K	K_H /bar C_2H_4	K_H /bar C_2H_2	$S_{C_2H_2/C_2H_4}$
50% C_2H_2 –50% C_2H_4	313.1	72.8 (± 1.0)	2.9 (± 0.1)	25.1
10% C_2H_2 –90% C_2H_4	298.1	51.5 (± 0.5)	1.4 (± 0.1)	36.8
	303.1	54.0 (± 0.2)	1.6 (± 0.1)	33.8
	308.1	56.6 (± 0.1)	2.0 (± 0.1)	28.3
	313.1	59.7 (± 0.1)	2.3 (± 0.1)	26.0

$$\Delta_{sol}G = RT \ln \left(\frac{K_H(T, p)}{p^0} \right) \quad (6)$$

$$\Delta_{sol}H = R \left(\frac{\partial \ln (K_H(T, p)/p^0)}{\partial (1/T)} \right)_p \quad (7)$$

$$\Delta_{sol}S = \left(\frac{\Delta_{sol}H - \Delta_{sol}G}{T} \right) \quad (8)$$

Based on the coefficient values obtained from Eq. 5, Gibbs free energy ($\Delta_{sol}G$), enthalpies ($\Delta_{sol}H$), and entropies ($\Delta_{sol}S$) of absorption were calculated using Eqs. 6–8 (results are shown in Table 5). The Gibbs free energies of C_2H_4 and C_2H_2 dissolving in the five ILs are all greater than zero and are positively correlated with the temperature change. More attention is paid to the values of enthalpy and entropy because it provides valuable information about the solute–solvent interactions and the molecular structure of the solutions. The enthalpy of the solution is closely related to the crossed solute–solvent molecular interactions and the entropy of solvation provides indications of the structure of the solvent molecules surrounding the solute.³⁶ As shown in Table 5, the solvation entropy of C_2H_4 and C_2H_2 in ILs is mainly negative, indicating that the solvation process is exothermic in the temperature range covered. This is accordance with the above experimental data that the solubility of C_2H_4 and C_2H_2 increases as temperature increases. In addition, the enthalpies and entropies of C_2H_2 solvation in ILs do not obviously change within the temperature ranges investigated. By contrast, the enthalpies and entropies of C_2H_4 solvation in ILs vary significantly with temperature. This is because the solvation resulted from the combination of various types of interactions. In the case of C_2H_2 , the strong H-bond interaction between C_2H_2 and IL is foremost in determining the solubility of C_2H_2 , which is less affected by the temperature; however, the solvation of C_2H_4 in ILs is a typical physical

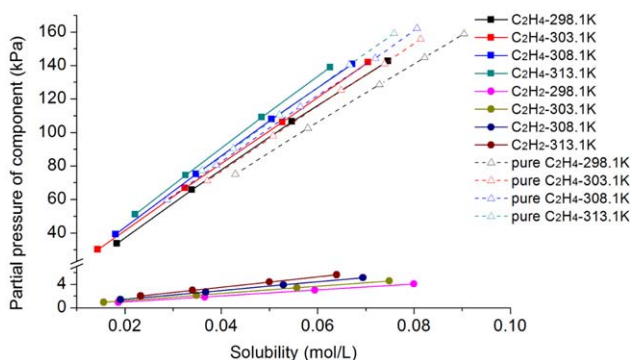


Figure 7. Solubility of mixture of 10% C_2H_2 and 90% C_2H_4 in $[P_{4444}][C_5COO]$.

[Color figure can be viewed in the online issue, which is available at wileyonlinelibrary.com.]

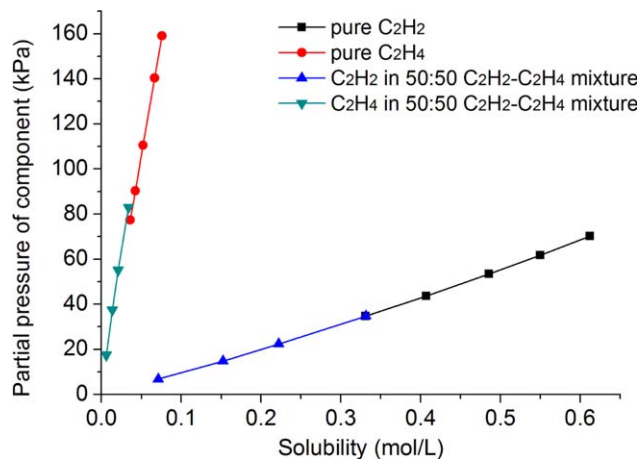


Figure 8. Solubility of pure gases and equimolar mixture of C_2H_2 and C_2H_4 in $[P_{4444}][C_5COO]$ at 313.1 K.

[Color figure can be viewed in the online issue, which is available at wileyonlinelibrary.com.]

absorption process in which a weak van der Waals interaction plays an important role. Therefore, the enthalpies and entropies of C_2H_4 solvation in ILs are more sensitive to temperature than C_2H_2 .

Separating performance for C_2H_2 – C_2H_4 mixture using $[P_{4444}][C_5COO]$

In practice, the real selectivity of C_2H_2 to C_2H_4 in IL may differ from the ideal selectivity calculated from the solubility data of pure gaseous solute on account of the complex interactions of gas mixture in IL. Thus, the separation performance of $[P_{4444}][C_5COO]$ was further evaluated using the mixture of C_2H_2 and C_2H_4 with different composition. One mixture contains equimolar C_2H_2 and C_2H_4 (50:50) and another mixture is a model cracking gas (10% C_2H_2 and 90% C_2H_4 , 10:90).

The solubility data were determined at temperature of 298.1 to 313.1 K and at total pressure of 20 to 150 kPa due to the limitation of experimental equipment. As the results shown in Table 6, the $[P_{4444}][C_5COO]$ demonstrated excellent separation selectivity to the mixture of C_2H_2 and C_2H_4 . With equimolar C_2H_2 – C_2H_4 mixture as feed gas, the real $S_{(C_2H_2/C_2H_4)}$ of $[P_{4444}][C_5COO]$ was up to 25.1 at 313.1K; while with model cracking gas (10:90), the real $S_{(C_2H_2/C_2H_4)}$ was 26.0 at 313.1 K and the value increased with decreasing temperature and topped out 36.8 at 298.1K, which were significantly higher than the ideal $S_{(C_2H_2/C_2H_4)}$ calculated from the solubility data of pure gases at the same temperature. Figures 7 and 8 showed the solubility data of C_2H_4 in $[P_{4444}][C_5COO]$ with 10:90 and 50:00 C_2H_2 – C_2H_4 mixture as feed gases, it is clear that the solubility of C_2H_4 in $[P_{4444}][C_5COO]$ with mixed gas as feed was slightly smaller than that with pure C_2H_4 at the same equilibrium partial pressure. It can be attributed to the competing absorption of C_2H_4 and C_2H_2 in $[P_{4444}][C_5COO]$, in which C_2H_2 has stronger interaction with IL and larger solubility than C_2H_4 . When the C_2H_2 molecules are hosted in the cavities or affiliating sites of the IL, the opportunity of IL interacting with C_2H_4 molecules reduces. Therefore, higher separation selectivity could be obtained with the mixture of C_2H_2 and C_2H_4 as feed gas.

It can also be seen in Figure 7 and 8 that the solubility of C_2H_2 increased with increasing the equilibrium partial

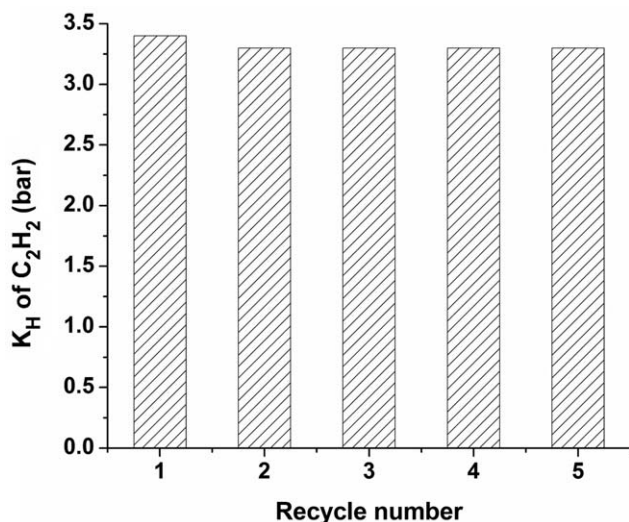


Figure 9. Recycled Henry's law constants tests of C₂H₂ in [P₄₄₄₄][C₅COO] at 313.1 K.

pressure of C₂H₂. At the same partial pressure (35 kPa, Figure 8), the solubility of C₂H₂ in IL with mixed gas had the similar value as pure C₂H₂. However, the K_{H,C_2H_2} calculated from the solubility data of 50:50 and 10:90 mixture was 2.9 and 2.3 bar at 313.1 K, respectively, which was smaller than the K_{H,C_2H_2} from pure C₂H₂ solubility data. It is because the solubility of C₂H₂ in [P₄₄₄₄][C₅COO] is very large (0.2 mol/mol at 70 kPa) which is far beyond the hypothesis of dilute solution; therefore the K_H was pressure-dependent according to the Krichevsky–Kasarnovsky equation.⁵⁴ The value of 2.9 bar for K_{H,C_2H_2} with 50:50 C₂H₂–C₂H₄ mixture was calculated from the C₂H₂ equilibrium partial pressure of 6.8–35 kPa, while the 3.3 bar for pure C₂H₂ was obtained from 35–70 kPa (detailed data in Supporting Information Tables S4 and S5). Similar experimental phenomenon was also observed in the physical absorption of CO₂ in ILs.⁵⁵

Although the total pressure of the cracking gas in industry is up to 0.8 MPa, the partial pressures of C₂H₂ and C₂H₄ are similar with the 10:90 C₂H₂–C₂H₄ mixture used in this study. Therefore, [P₄₄₄₄][C₅COO] has the great potential in separating C₂H₂ from C₂H₄ in cracking gas.

Recycle test of C₂H₂ absorption

The absorption/desorption recycling of an absorbent is a critical property for gas absorption. The recycling performance of [P₄₄₄₄][C₅COO], which has the highest mass capacity for C₂H₂, was evaluated using pure C₂H₂ as feed gas. After absorption, the IL was degassed under a vacuum at 343 K. The results from five absorption–desorption cycles are shown in Figure 9. It is clear that the K_{H,C_2H_2} in the IL was maintained well during the five cycles. Therefore, this recycling experiment demonstrated that the C₂H₂–IL binding is reversible and the IL, [P₄₄₄₄][C₅COO], can be regenerated without a loss in IL and capacity for C₂H₂.

Conclusions

In this study, a screening method is proposed for the molecular design of ILs to separate C₂H₂ from C₂H₄, which is based on the prediction of the K_H by using the COSMO-RS method. Combining 15 cations and 28 anions, 420 ILs are screened to find promising candidates to separate C₂H₂

from C₂H₄. The screening results show that the structure of anions plays a key role in the ILs' separation selectivity and capacity, and the structure of cations also has a significant influence on the capacity of C₂H₂ in ILs. Based on the results of COSMO-RS calculations, a type of tetraalkylphosphonium-based ILs with long-chain carboxylate anions were designed for C₂H₂/C₂H₄ separation.

The solubility's of C₂H₂ and C₂H₄ in several tetraalkylphosphonium-based ILs, including [P₄₄₄₄][C₅COO], [P₄₄₄₄][C₇COO], [P₆₆₆₍₁₄₎][OAc], [P₆₆₆₍₁₄₎][Pyr], and [P₆₆₆₍₁₄₎][Oxa], were determined at temperatures of 298.1 to 313.1 K and pressures of 20 to 160 kPa. The experimental data showed that the tetraalkylphosphonium-based IL with long-chain carboxylate anion [P₄₄₄₄][C₅COO] shows excellent absorption performance for C₂H₂, the K_{H,C_2H_2} reaches 2.1 bar and the separation selectivity is up to 21.4 at 298.1 K. Furthermore, the ILs could be regenerated easily by heating or vacuum desorption. The solubility of binary gas mixtures containing C₂H₂ and C₂H₄ was measured, and the real selectivity of C₂H₂ to C₂H₄ for simulated typical cracking gas mixture (10% C₂H₂ and 90% C₂H₄ mixture) could reach 36.8 at 298.1 K. Therefore, [P₄₄₄₄][C₅COO] shows great potential in separating C₂H₂ from C₂H₄.

The results of this work show that introducing a flexible and highly asymmetric structure and simultaneously enhancing the H-bond basicity of anions in ILs is an efficient method for obtaining high capacity and good selectivity of C₂H₂ in ILs. We believe that this method is also significant for the separation of other acidic gases, such as CO₂, H₂S, and SO₂.

Acknowledgments

The authors are grateful for the financial supports from the National Natural Science Foundation of China (21222601, 21436010), the Zhejiang Provincial Natural Science Foundation of China (LR13B060001) and the Program for New Century Excellent Talents in University (NCET-13-0524).

Literature Cited

- Yashima E, Matsushima T, Okamoto Y. Chirality assignment of amines and amino alcohols based on circular dichroism induced by helix formation of a stereoregular poly((4-carboxyphenyl)acetylene) through acid–base complexation. *J Am Chem Soc.* 1997;119:6345–6359.
- Silvestri F, Marrocchi A. Acetylene-based materials in organic photovoltaics. *Int J Mol Sci.* 2010;11:1471–1508.
- Pässler P, Hefner W, Buckl K, Meinass H, Meiswinkel A, Wernicke HJ, Ebersberg G, Müller R, Bässler J, Behringer H. *Acetylene*. Weinheim: Wiley-VCH, 2008.
- Bereshnaya KP, Bystrova TA, Zelentsova NI, Avrekh GI, Shamrai OB. Recovery and utilization of by-product acetylene from olefin production. *Chem Tech Fuels Oil.* 1979;15:756–757.
- Weissermel K, Arpe HJ. *Industrial Organic Chemistry*, 4th edition. Weinheim: Wiley-VCH, 2003:313–336.
- Yang RT, Kikkides ES. New sorbents for olefin/paraffin separations by adsorption via π -complexation. *AIChE J.* 1995;41:509–517.
- Rege SU, Padin J, Yang RT. Olefin/paraffin separations by adsorption: π -complexation vs. kinetic separation. *AIChE J.* 1998;44:799–809.
- Xiang S, Zhang Z, Zhao C, Hong K, Zhao X, Ding D, Xie M, Wu C, Das MC, Gill R. Rationally tuned micropores within enantiopure metal-organic frameworks for highly selective separation of acetylene and ethylene. *Nat Commun.* 2011;2:204.
- Matsuda R, Kitaura R, Kitagawa S, Kubota Y, Belosludov RV, Kobayashi TC, Sakamoto H, Chiba T, Takata M, Kawazoe Y. Highly controlled acetylene accommodation in a metal-organic microporous material. *Nature.* 2005;436:238–241.

10. Ruta M, Laurenczy G, Dyson PJ, Kiwi-Minsker L. Pd nanoparticles in a supported ionic liquid phase: highly stable catalysts for selective acetylene hydrogenation under continuous-flow conditions. *J Phys Chem C*. 2008;112:17814–17819.
11. Kovnir K, Armbrüster M, Teschner D, Venkov TV, Szentmiklósi L, Jentoft FC, Knop-Gericke A, Grin Y, Schlögl R. In situ surface characterization of the intermetallic compound PdGa - A highly selective hydrogenation catalyst. *Surf Sci*. 2009;603:1784–1792.
12. Welton T. Room-temperature ionic liquids. Solvents for synthesis and catalysis. *Chem Rev*. 1999;99:2071–2084.
13. Camper D, Bara JE, Gin DL, Noble RD. Room-temperature ionic liquid–amine solutions: tunable solvents for efficient and reversible capture of CO₂. *Ind Eng Chem Res*. 2008;47:8496–8498.
14. Hu Y, Liu Z, Xu C, Zhang X. The molecular characteristics dominating the solubility of gases in ionic liquids. *Chem Soc Rev*. 2011;40:3802–3823.
15. Pinto AM, Rodríguez H, Colón YJ, Arce AJ, Arce A, Soto A. Absorption of carbon dioxide in two binary mixtures of ionic liquids. *Ind Eng Chem Res*. 2013;52:5975–5984.
16. Shiflett MB, Shiflett AD, Yokozeki A. Separation of tetrafluoroethylene and carbon dioxide using ionic liquids. *Sep Purif Technol*. 2011;79:357–364.
17. Shiflett MB, Yokozeki A. Separation of carbon dioxide and sulfur dioxide using room-temperature ionic liquid [bmim][MeSO₄]. *Energ Fuel*. 2009;24:1001–1008.
18. Moura L, Mishra M, Bernalles V, Fuentealba P, Padua AAH, Santini CC, Costa Gomes MF. Effect of unsaturation on the absorption of ethane and ethylene in imidazolium-based ionic liquids. *J Phys Chem B*. 2013;117:7416–7425.
19. Palgunadi J, Kim HS, Lee JM, Jung S. Ionic liquids for acetylene and ethylene separation: Material selection and solubility investigation. *Chem Eng Process*. 2010;49:192–198.
20. Lee JM, Palgunadi J, Kim JH, Jung S, Choi Y, Cheong M, Kim HS. Selective removal of acetylenes from olefin mixtures through specific physicochemical interactions of ionic liquids with acetylenes. *Phys Chem Chem Phys*. 2010;12:1812–1816.
21. Palgunadi J, Hong SY, Lee JK, Lee H, Lee SD, Cheong M, Kim HS. Correlation between hydrogen bond basicity and acetylene solubility in room temperature ionic liquids. *J Phys Chem B*. 2011;115:1067–1074.
22. Zhao X, Xing H, Yang Q, Li R, Su B, Bao Z, Yang Y, Ren Q. Differential solubility of ethylene and acetylene in room-temperature ionic liquids: a theoretical study. *J Phys Chem B*. 2012;116:3944–3953.
23. Xing H, Zhao X, Yang Q, Su B, Bao Z, Yang Y, Ren Q. Molecular dynamics simulation study on the absorption of ethylene and acetylene in ionic liquids. *Ind Eng Chem Res*. 2013;52:9308–9316.
24. Holbrey JD, Seddon KR. Ionic liquids. *Clean Prod Proc*. 1999;1:223–236.
25. Klamt A. Conductor-like screening model for real solvents: a new approach to the quantitative calculation of solvation phenomena. *J Phys Chem*. 1995;99:2224–2235.
26. Diedenhofen M, Eckert F, Klamt A. Prediction of infinite dilution activity coefficients of organic compounds in ionic liquids using COSMO-RS. *J Chem Eng Data*. 2003;48:475–479.
27. Banerjee T, Khanna A. Infinite dilution activity coefficients for trihexyltetradecyl phosphonium ionic liquids: measurements and COSMO-RS prediction. *J Chem Eng Data*. 2006;51:2170–2177.
28. Manan NA, Hardacre C, Jacquemin J, Rooney DW, Youngs TG. Evaluation of gas solubility prediction in ionic liquids using COSMOthermX. *J Chem Eng Data*. 2009;54:2005–2022.
29. Maiti A. Theoretical screening of ionic liquid solvents for carbon capture. *ChemSusChem*. 2009;2:628–631.
30. Zhang X, Liu Z, Wang W. Screening of ionic liquids to capture CO₂ by COSMO-RS and experiments. *AIChE J*. 2008;54:2717–2728.
31. Gonzalez-Miquel M, Palomar J, Omar S, Rodriguez F. CO₂/N₂ selectivity prediction in supported ionic liquid membranes (SILMs) by COSMO-RS. *Ind Eng Chem Res*. 2011;50:5739–5748.
32. Xing H, Zhao X, Li R, Yang Q, Su B, Bao Z, Yang Y, Ren Q. Improved efficiency of ethylene/ethane separation using a symmetrical dual nitrile-functionalized ionic liquid. *ACS Sustainable Chem Eng*. 2013;1:1357–1363.
33. Mortazavi-Manesh S, Satyro MA, Marriott RA. Screening ionic liquids as candidates for separation of acid gases: solubility of hydrogen sulfide, methane, and ethane. *AIChE J*. 2013;59:2993–3005.
34. Yang Q, Xing H, Su B, Bao Z, Wang J, Yang Y, Ren Q. The essential role of hydrogen-bonding interaction in the extractive separation of phenolic compounds by ionic liquid. *AIChE J*. 2013;59:1657–1667.
35. Camper D, Scovazzo P, Koval C, Noble R. Gas solubilities in room-temperature ionic liquids. *Ind Eng Chem Res*. 2004;43:3049–3054.
36. Jacquemin J, Costa Gomes MF, Husson P, Majer V. Solubility of carbon dioxide, ethane, methane, oxygen, nitrogen, hydrogen, argon, and carbon monoxide in 1-butyl-3-methylimidazolium tetrafluoroborate between temperatures 283K and 343K and at pressures close to atmospheric. *J Chem Thermodynamics*. 2006;38:490–502.
37. Dymond JH, Marsh KN, Wilhoit RC, Wong KC. *Virial Coefficients of Pure Gases and Mixtures*. In: Frenkel, M., Marsh, K. N., editors. Berlin: Springer-Verlag, 2002.
38. Ahlrichs R, Bär M, Häser M, Horn H, Kölmel C. Electronic structure calculations on workstation computers: The program system turbomole. *Chem Phys Lett*. 1989;162:165–169.
39. Becke AD. Density-functional exchange-energy approximation with correct asymptotic behavior. *Phys Rev A*. 1988;38:3098.
40. Perdew JP. Density-functional approximation for the correlation energy of the inhomogeneous electron gas. *Phys Rev B*. 1986;33:8822–8824.
41. Schäfer A, Huber C, Ahlrichs R. Fully optimized contracted gaussian basis sets of triple zeta valence quality for atoms Li to Kr. *J Chem Phys*. 1994;100:5829.
42. Eckert F, Klamt A. *COSMOtherm*, Version C3.0, Release 12.01; COSMOlogic GmbH & Co. KG, Leverkusen, Germany, 2012.
43. Lee JM, Palgunadi J, Kim JH, Jung S, Choi Y, Cheong M, Kim HS. Selective removal of acetylenes from olefin mixtures through specific physicochemical interactions of ionic liquids with acetylenes. *Phys Chem Chem Phys*. 2010;12:1812–1816.
44. Fallanza M, González-Miquel M, Ruiz E, Ortiz A, Gorri D, Palomar J, Ortiz I. Screening of RTILs for propane/propylene separation using COSMO-RS methodology. *Chem Eng J*. 2013;220:284–293.
45. Xu D, Yang Q, Su B, Bao Z, Ren Q, Xing H. Enhancing the basicity of ionic liquids by tuning the cation-anion interaction strength and via the anion-ethered strategy. *J Phys Chem B*. 2014;118:1071–1079.
46. Almeida HFD, Passos H, Lopes-da-Silva JA, Fernandes AM, Freire MG, Coutinho JAP. Thermophysical properties of five acetate-based ionic liquids. *J Chem Eng Data*. 2012;57:3005–3013.
47. Pässler P, Hefner W, Buckl K, Meinass H, Meiswinkel A, Wernicke H, Ebersberg G, Müller R, Bässler J, Behringer H, Mayer D. *Acetylene*. Wiley-VCH Verlag GmbH & Co. KGaA, 2000:5.
48. Jacquemin J, Husson P, Majer V, Gomes MFC. Low-pressure solubilities and thermodynamics of solvation of eight gases in 1-butyl-3-methylimidazolium hexafluorophosphate. *Fluid Phase Equilib*. 2006;240:87–95.
49. Husson-Borg P, Majer V, Costa Gomes MF. Solubilities of oxygen and carbon dioxide in butyl methyl imidazolium tetrafluoroborate as a function of temperature and at pressures close to atmospheric pressure. *J Chem Eng Data*. 2003;48:480–485.
50. Hong G, Jacquemin J, Deetlefs M, Hardacre C, Husson P, Costa Gomes MF. Solubility of carbon dioxide and ethane in three ionic liquids based on the bis {(trifluoromethyl) sulfonyl} imide anion. *Fluid Phase Equilib*. 2007;257:27–34.
51. Soriano AN, Doma BT Jr, Li M. Solubility of carbon dioxide in 1-ethyl-3-methylimidazolium 2-(2-methoxyethoxy) ethylsulfate. *J Chem Thermodynamics*. 2008;40:1654–1660.
52. Soriano AN, Doma BT Jr, Li M. Carbon dioxide solubility in 1-ethyl-3-methylimidazolium trifluoromethanesulfonate. *J Chem Thermodynamics*. 2009;41:525–529.
53. Jalili AH, Mehdizadeh A, Shokouhi M, Sakhaeinia H, Taghikhani V. Solubility of CO₂ in 1-(2-hydroxyethyl)–3-methylimidazolium ionic liquids with different anions. *J Chem Thermodynamics*. 2010;42:787–791.
54. Krichevsky IR, Kasarnovsky JS. Thermodynamical calculations of solubilities of nitrogen and hydrogen in water at high pressures. *J Am Chem Soc*. 1935;57:2168–2171.
55. Anthony JL, Anderson JL, Maginn EJ, Brennecke JF. Anion effects on gas solubility in ionic liquids. *J Phys Chem B*. 2005;109:6366–6374.

Manuscript received July 29, 2014, and revision received Jan. 24, 2015.